Physics Letters B 789 (2019) 300–307

Contents lists available at ScienceDirect

Physics Letters B

www.elsevier.com/locate/physletb

Rapidity gap survival factors caused by remnant fragmentation for W^+W^- pair production via $\gamma^*\gamma^* \to W^+W^-$ subprocess with photon transverse momenta

Laurent Forthomme [a], Marta Łuszczak [b,*], Wolfgang Schäfer [c], Antoni Szczurek [c,*]

[a] Institute of Physics and Astronomy, The University of Kansas, Lawrence, USA [1]
[b] Faculty of Mathematics and Natural Sciences, University of Rzeszów, ul. Pigonia 1, PL-35-310 Rzeszów, Poland
[c] Institute of Nuclear Physics Polish Academy of Sciences, ul. Radzikowskiego 152, PL-31-342 Kraków, Poland

ARTICLE INFO

Article history:
Received 28 May 2018
Received in revised form 26 November 2018
Accepted 10 December 2018
Available online 21 December 2018
Editor: B. Grinstein

ABSTRACT

We calculate the cross section for $pp \to W^+W^-$ in the recently developed k_T-factorisation approach, including transverse momenta of the virtual photons. We focus on processes with single and double proton dissociation. First we discuss the gap survival on the parton level as due to the emission of extra jet. Both the role of valence and sea contributions is discussed. The hadronisation of proton remnants is performed with PYTHIA 8 string fragmentation model, assuming a simple quark–diquark model for proton. Highly excited remnant systems hadronise producing particles that can be vetoed in the calorimeter. We calculate associated effective gap survival factors. The gap survival factors depend on the process, mass of the remnant system and collision energy. The rapidity gap survival factor due to remnant fragmentation for double dissociative (DD) collisions ($S_{R,DD}$) is smaller than that for single dissociative (SD) process ($S_{R,SD}$). We observe the approximate factorisation $S_{R,DD} \approx (S_{R,SD})^2$, however it is expected that this property will be violated by soft rescattering effects not accounted for in this letter.

1. Introduction

The processes with partonic $\gamma\gamma \to O_1O_2$ (O_1 and O_2 being electroweak states) subprocesses become recently very topical. Experimentally they can be separated from other competing processes by imposing rapidity gaps around the electroweak vertex. Both charged lepton pairs l^+l^- [1–5] and electroweak gauge bosons W^+W^- [6,7] were recently studied experimentally at the Large Hadron Collider. In particular processes with W^+W^- are of special interest as here one can study e.g. anomalous quartic gauge boson couplings [8,9]. Precise data may therefore provide a useful information allowing to test the Standard Model in a sector, which is so far not accessible otherwise.

There are, in general, different categories of such processes depending on whether the proton stays intact or undergoes an electromagnetic dissociation (see e.g. [10,11]).

The W^+W^- production in proton–proton processes via the $\gamma\gamma \to W^+W^-$ subprocess was recently studied in collinear [12] and transverse momentum dependent factorisation [13] approaches.

Without additional requirements it is impossible to separate the $\gamma\gamma \to W^+W^-$ mechanism from $q\bar{q} \to W^+W^-$, $gg \to W^+W^-$ or higher-order QCD processes. To enhance the sample for the wanted mechanism one may impose a rapidity gap condition around e.g. the $e^+\mu^-$ or $e^-\mu^+$ vertex in the leptonic decay of the central diboson system.

In Fig. 1 we show a schematic picture of the single and double dissociative two-photon processes. In our recent paper [13] we have shown that rather large photon virtualities and large mass proton excitation are characteristic for the $\gamma\gamma \to W^+W^-$ induced processes. The highly excited hadronic systems hadronise producing (charged) particles that may destroy the rapidity gap around the central event vertex. The minimal requirement is to impose a condition of no charged particles in the main ATLAS or CMS trackers.

We will focus on such effects in the present letter. The hadronisation of the proton remnants will be performed and conditions on charged particles will be imposed. Our main aim is to estimate gap

* Corresponding authors.
E-mail addresses: laurent.forthomme@cern.ch (L. Forthomme), luszczak@ur.edu.pl (M. Łuszczak), wolfgang.schafer@ifj.edu.pl (W. Schäfer), antoni.szczurek@ifj.edu.pl (A. Szczurek).
[1] Now at Helsinki Institute of Physics, University of Helsinki, Finland.

https://doi.org/10.1016/j.physletb.2018.12.018

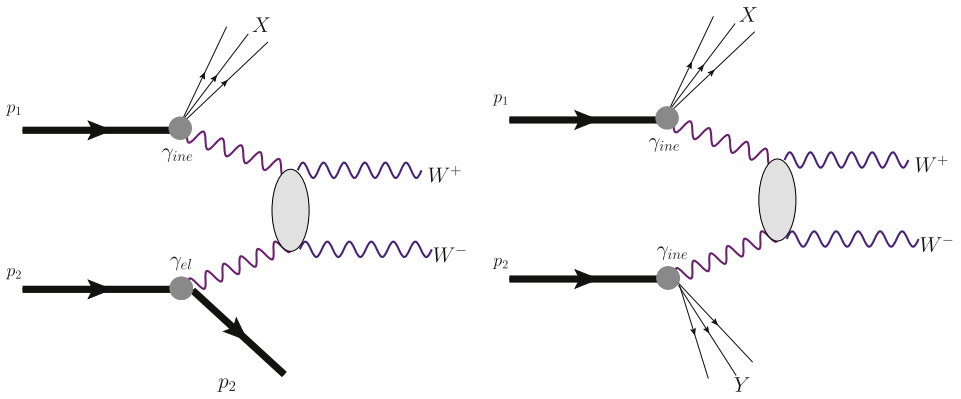

Fig. 1. The single and double dissociative mechanisms discussed in the present letter.

survival factor associated with the remnant hadronisation, which destroys the rapidity gap. Dependence on kinematic variables will be studied.

As has been stressed in [14], the ordinary collinear photon parton distribution functions (PDFs) – which imply a fully inclusive sum over remnant final states – cannot be used if additional gap requirements are imposed on the final states. For this purpose, in Ref. [14] a concept of "photon PDF in events with rapidity gaps" was introduced. There a requirement, that the parton emissions related to evolution do not contaminate the central rapidity region is implemented. The authors tried to approximately modify the collinear photon PDF to include rapidity gap requirement(s) used in modern experiments. The calculations in [14] are kept at the parton level, and no explicit remnant hadronisation effects were discussed there.

The effect of gap survival related to the remnant fragmentation was discussed previously in the context of the e^+e^- central production in the framework of the LPAIR code [15].

Remnant fragmentation is not the only effect that can destroy the rapidity gap. There are also possible interactions between the spectator partons of the colliding protons [16]. The gap survival factors for these processes are beyond the scope of the present letter. For recent estimates in photon induced processes, see e.g. [14, 17,18]. While [14] discusses results at parton level it does include soft processes when calculating a gap survival factor.

Within our approach the consistent inclusion of soft survival effects remains a pressing issue for the future.

2. Sketch of our calculational scheme

We calculate cross section for the $pp \to W^+W^-$ reaction with double proton dissociation as:

$$\begin{aligned}\frac{\mathrm{d}\sigma(pp\to XW^+W^-Y)}{\mathrm{d}y_+\mathrm{d}y_-\mathrm{d}^2\mathbf{p}_\perp^+\mathrm{d}^2\mathbf{p}_\perp^-\mathrm{d}M_X\mathrm{d}M_Y} &= x_1x_2\int d^2\mathbf{k}_{1\perp}d^2\mathbf{k}_{2\perp}\frac{\mathrm{d}\gamma(x_1,\mathbf{k}_{1\perp},M_X)}{\mathrm{d}M_X}\frac{\mathrm{d}\gamma(x_2,\mathbf{k}_{2\perp},M_Y)}{\mathrm{d}M_Y}\times\\ &\times\frac{1}{16\pi^2(x_1x_2s)^2}\sum_{\lambda_{W^+}\lambda_{W^-}}|M(\lambda_{W^+},\lambda_{W^-};\mathbf{k}_{1\perp},\mathbf{k}_{2\perp})|^2\\ &\times\delta^{(2)}(\mathbf{p}_\perp^+ + \mathbf{p}_\perp^- - \mathbf{k}_{1\perp} - \mathbf{k}_{2\perp}).\end{aligned} \tag{2.1}$$

Here $y_\pm$ are the rapidities and $\mathbf{p}_\perp^\pm$ the transverse momenta of $W^\pm$ bosons. The M_X-dependent photon fluxes can be decomposed into fluxes corresponding to the relevant proton staying intact or dissociating (see Fig. 1):

$$\begin{aligned}\frac{\mathrm{d}\gamma(x_1,\mathbf{k}_{1\perp},M_X)}{\mathrm{d}M_X} &= \gamma_{\mathrm{el}}(x_1,\mathbf{k}_{1\perp})\delta(M_X-m_p)\\ &+\frac{\mathrm{d}\gamma_{\mathrm{inel}}(x_1,\mathbf{k}_{1\perp},M_X)}{\mathrm{d}M_X}\theta\big(M_X-(m_p+m_\pi)\big),\end{aligned} \tag{2.2}$$

and similarly for $(x_1,\mathbf{k}_{1\perp},M_X)\leftrightarrow(x_2,\mathbf{k}_{2\perp},M_Y)$, so that the cross section for single dissociative process is less differential as one of the two integrations over the remnant masses is unnecessary. Such photon fluxes can be understood as a type of unintegrated parton distributions [19]. They allow us to generate events containing remnants of mass M_X, M_Y. Details on the relation of photon fluxes to proton structure functions and the used matrix element $M(\lambda_{W^+},\lambda_{W^-};\mathbf{k}_{1\perp},\mathbf{k}_{2\perp})$ can be found in [13] and references therein.

Let us briefly recall the main ingredients for the construction of photon fluxes. Elastic pieces only require the standard electromagnetic form factors of a proton. The inelastic fluxes need the proton structure functions $F_2(x_{\mathrm{Bj}},Q^2)$ and $F_L(x_{\mathrm{Bj}},Q^2)$. We use a parameterisation of F_2 and F_L, which incorporates a large body of experimental data available in different regions of x_{Bj}, Q^2. For $Q^2 > 9$ GeV^2 it uses a perturbative QCD NNLO calculation [20], while in the domain $Q^2 < 9$ GeV^2 the resonance region is described by a fit found in [21], and elsewhere by the parameterisation of [22]. For the longitudinal structure function, [23] is used to supplement [22].

We use an implementation of the above process in CepGen [24] for the Monte Carlo generation of unweighted events.

The hadronisation of remnant states X and/or Y is performed using the Lund fragmentation algorithm implemented in PYTHIA 8 [25], and interfaced to CepGen. We model the incoming photon as emitted from a valence (up) quark collinear to the incoming proton direction. Other flavour combinations are also expected to contribute to the process, but we observe the kinematics of the outgoing X and Y systems is not sensitive to this choice. The fractional quark momentum x_{Bj} is determined event-by-event from the photon virtuality Q^2 and the relevant remnant mass M_X through:

$$x_{\mathrm{Bj}} = \frac{Q^2}{Q^2+M_X^2-m_p^2}.$$

We check the condition for each "stable" (pions, kaons, protons, ...) charged particle produced in the hadronisation of X and Y remnants:

$$-\eta_{\mathrm{cut}} < \eta^{\mathrm{ch}} < +\eta_{\mathrm{cut}}\,. \tag{2.3}$$

Each event for which at least one charged particle fulfils condition (2.3) is discarded. We introduce the ratio:

$$S_R(\omega) = \frac{N_{\text{accepted}}(\omega)}{N_{\text{all}}(\omega)}\,, \tag{2.4}$$

where ω denotes a set of kinematic variables describing details of the reaction. $S_R(\omega)$ can be considered a phase-space-point-dependent rapidity gap survival factor associated with remnant(s) fragmentation. For example we will show such number for different ranges of masses of the produced system both for double and single dissociation.

3. Numerical results

Here we wish to present some results of our Monte Carlo simulations. We consider separately the case of double dissociation as well as the case of single dissociation. The most important ingredient of our calculation is a realistic hadronisation of proton remnants, which allows to estimate the gap survival factor associated with spoiling the rapidity gap in the central pseudorapidity region. We assume a realistic situation $-2.5 < \eta < 2.5$, for individual (charged!) particles, relevant for recent CMS [6] and ATLAS [7] measurements.

It was shown e.g. in [13] that without any gap survival effects:

$$\sigma(\text{inel.-inel.}) > \sigma(\text{inel.-el.}) + \sigma(\text{el.-inel.}) > \sigma(\text{el.-el.})\,. \tag{3.1}$$

Can this ordering be changed when the rapidity gap requirement is taken into account? As will be shown below, suppression effects (due to emission of a jet and the remnant fragmentation) are the biggest for inelastic–inelastic processes, so that in principle the ordering in (3.1) can be changed when a rapidity veto is imposed.

An important caveat has to be added: spectator parton rescatterings can also change the hierarchy of (3.1). Indeed, it is understood that these soft interactions will strongly depend on the centrality of the collision in impact parameter space [16]. Photon exchange is generally long range in impact parameter space, but events with large virtualities $Q^2_{1,2}$ will be rather central and thus be more affected by spectator rescatterings.

3.1. Parton level approach for single dissociation

Before studying the hadron level we wish to calculate the gap survival factor on the parton level. In such a case it is the outgoing parton (jet or mini-jet), which is struck by the virtual photon and destroys the rapidity gap.

The gap survival factor can be then defined as:

$$S_R(\eta_{\text{cut}}) = 1 - \frac{1}{\sigma}\int\limits_{-\eta_{\text{cut}}}^{\eta_{\text{cut}}} \frac{\mathrm{d}\sigma}{\mathrm{d}\eta_{\text{jet}}}\mathrm{d}\eta_{\text{jet}}, \tag{3.2}$$

where $\mathrm{d}\sigma/\mathrm{d}\eta_{\text{jet}}$ is the rapidity distribution of the cross section for W^+W^- production as a function of rapidity of the extra jet (*de facto* parton) and σ is the associated integrated cross section. In Fig. 2 we show $\mathrm{d}\sigma/\mathrm{d}\eta_{\text{jet}}$ as a function of η_{jet}. No extra cuts are imposed here. We get a very broad distribution in η_{jet} (see solid line).

Different processes contribute to this distribution: the jet may originate from the valence or sea (anti-)quark distribution. Unfortunately the NNLO calculation [20] does not allow a straightforward decomposition into sea and valence.

However, a leading-order parameterisation may be used to disentangle the partonic contribution to $F_2(x_{\text{Bj}}, Q^2)$ for $Q^2 > 9$ GeV^2. For illustration we show the contributions of valence (dashed line) and sea (dotted line) components in Fig. 2. As can be seen, rapidity distributions for different components are very different. The sea component is important for larger rapidities than the valence one.

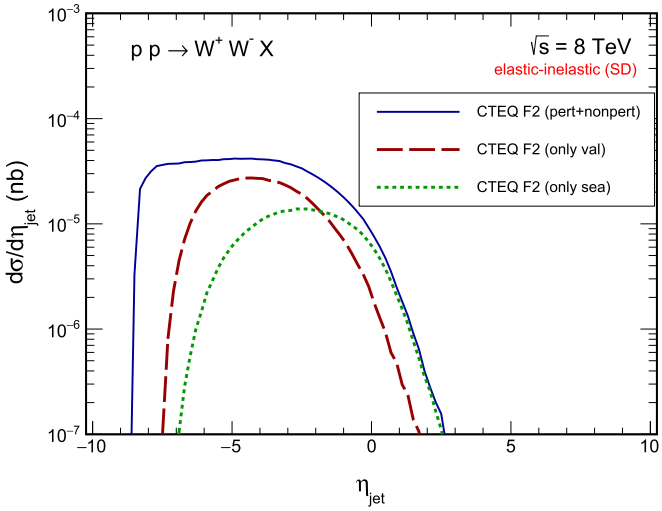

Fig. 2. Jet rapidity distribution for F_2 using a LO partonic distribution at large Q^2. The solid line is a sum of all contributions. The dashed line is for the valence component and the dotted line is for the sea component.

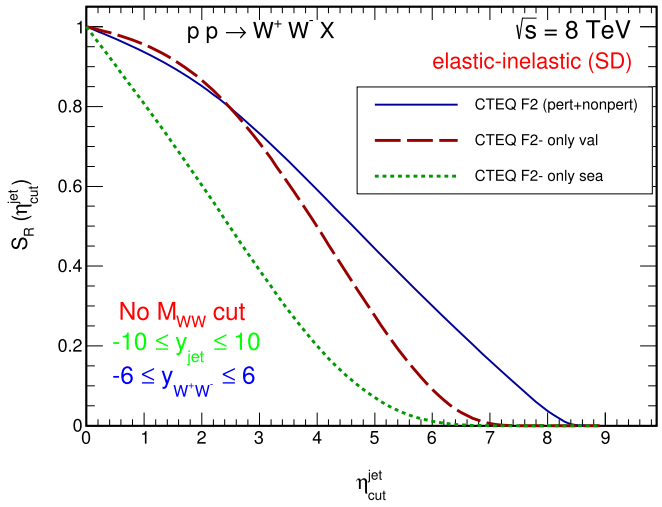

Fig. 3. Gap survival factor associated with the jet emission and defined by Eq. (3.2). The solid line is for the full model, the dashed line for the valence contribution and the dotted line for the sea contribution.

There is also a non-perturbative component at very negative rapidities. Notice that we generate events which include remnants of masses M_X, M_Y. All information on the excitation of these states is encoded in the proton structure functions F_2, F_L, taken essentially from data. In particular, it includes the excitation of baryon resonances and low-mass hadronic continua. The regions of low values of (Q_1^2) and/or $Q_2^2)$ are called nonperturbative as there the partonic picture is not enough. Our approach to the final state is very different from the one using collinear factorized partons, where an inclusive sum over all baryon remnants is implied. It is only after such an inclusive sum that the nonperturbative contribution at low Q^2 in our parametrization could be reexpressed in terms of the initial condition of "DGLAP" photons. Clearly this is not useful for the problem at hand.

Now we shall present the parton level gap survival factor as a function of the somewhat artificial window $(-\eta_{cut}, \eta_{cut})$ which is free of the outgoing parton (jet). We show corresponding $S_R(\eta_{cut})$ in Fig. 3. The solid line represents our partonic result. For comparison we show also S_R when only one component (valence or sea) of F_2 is included in the calculation, see dashed and dotted lines.

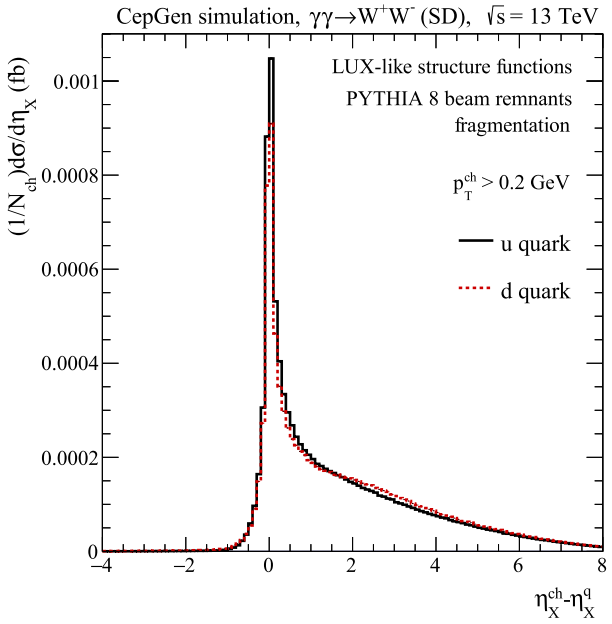

Fig. 4. Distribution of charged particles in the single dissociative case for u (black solid line) and d (red dotted line) quarks at 13 TeV with respect to η_{jet}.

In this case, the cross section σ in the denominator of Eq. (3.2) is the integral of the relevant component (sea or valence) only. We see that gap survival factors for the different components are fairly different. Our final result (solid line) correctly includes all components. Please notice that according to Eq. (3.2) the solid line is not the sum of the dashed and dotted curves. The distribution of S_R for the full model (solid curve) extends to much larger η_{cut} than the valence and sea contributions separately. This is due to a non-perturbative contribution (see a comment above), which dominates at very large negative rapidities (see the η_{jet} distribution in Fig. 2). The emitted jets can be associated only with partonic component of the model structure function.

3.2. Particles in the jet

Now we wish to show pseudorapidity distribution of charged particles relative to the parton (jet) rapidity ($\Delta\eta = \eta_{\text{ch}} - \eta_{\text{jet}}$). In Fig. 4 we see a sharp peak relative to zero which can be interpreted as the distribution within the jet. To the right of the peak we see in addition the contribution of beam remnants which leads to a visible asymmetry of the distribution. This means that the corresponding gap survival factor should be very similar when using the particle closest in rapidity space to the central system as that when using (pseudo)rapidity of the jet (parton). The effect of hadronisation is an order of magnitude smaller than the effect for different components (valence, sea, etc.).

3.3. Double dissociation

We start the detailed studies on the hadron level (including hadronisation) from the largest contribution, in the inclusive case, the inelastic–inelastic (double dissociative) [13] processes. In this case both remnants fragment and we have to include their fragmentation simultaneously. In Fig. 5 we show two-dimensional distributions in pseudorapidity of particles from X (η_X^{ch}) and Y (η_Y^{ch}) for different ranges of masses of the centrally produced system. For illustration the region relevant for ATLAS and CMS pseudorapidity coverage is pictured by the thin dashed square.

The two dimensional plots are not sufficient to see a dependence of the associated gap survival factor on the mass of the centrally produced system.

We quantify this effect, see Table 1, by showing average remnant rapidity gap factors for different ranges of M_{WW} masses. There we observe a mild dependence. The remnant rapidity gap survival factor at fixed η_{cut} becomes larger at higher collision energies.

In Fig. 6 we show the distribution in η_{cut} for the double dissociation process. We predict a strong dependence on η_{cut}. It would be valuable to perform experimental measurements with different η_{cut}.

3.4. Single dissociation

We repeat a similar analysis for the single dissociative process. In Fig. 7 we show the rapidity distribution of charged particles produced in the fragmentation of the X system. The contamination of the detector is only weakly correlated with the mass of the centrally produced system.

Again we quantify the effect by showing the average remnant rapidity gap survival factor for the same windows of M_{WW}. The conclusions here are similar as for the double dissociation, except that the effect of destroying the rapidity gap is smaller.

In Table 1 we show the rapidity gap survival factor for single and double dissociation processes. The middle column shows the square of single dissociation survival factors. By comparing the latter results with the ones for double dissociation, collected in Table 1 we observe that with good precision:

$$S_{R,DD} \approx \left(S_{R,SD}\right)^2 . \tag{3.3}$$

Such an effect is naively expected when the two fragmentations are independent, which is the case by the model construction. Again, we repeat the caveat, that soft processes will violate the factorisation discussed here.

In Fig. 8 we show the distribution in η_{cut} for single dissociative process. The numbers here are somewhat larger than those shown in Fig. 6, consistently with factorisation. Detailed inspection shows (3.3) holds for all M_{WW} regions.

For later studies, the dependence of the rapidity gap survival factor on the mass of the dissociated hadronic system may be interesting. Corresponding results are shown in Fig. 9. We observe that for an η_{cut} value of 2.5 the rapidity gap survival factor S_R stays very close to 1 for $M_X^{\text{max}} < 100$ GeV. Increasing the mass of the dissociative system leads to graduate destroying of the (pseudo)rapidity gap, arbitrarily fixed here to $-2.5 < \eta < 2.5$ (ATLAS, CMS).

From Fig. 9 one may infer which masses can be allowed in the dissociation still ensuring the gap and avoiding a more complicated Monte Carlo simulation of the remnant hadronisation.

The hadronisation part depends on the kinematics of the centrally produced system, but otherwise is independent of the quantum numbers of this system. Hence, this method can be used to perform calculations for processes for which there are no direct procedures to perform full Monte Carlo simulations.

Let us come back to the ordering of different processes (3.1). In Table 2 we show the relative contributions of exclusive (Exc.), single dissociative (SD) and double dissociative (DD) processes for the inclusive case (without gap requirement) as well as for $\eta_{\text{cut}} = 2.5$ and $\eta_{\text{cut}} = 6.5$. Similar results are shown in Table 3 of [14] (their $\delta = 3$ and $\delta = 7$ correspond to our $\eta_{\text{cut}} = 6.5$ and $\eta_{\text{cut}} = 2.5$, respectively), including effects of soft rescatterings in a simple two-channel eikonal model. It can be seen that for $\eta_{\text{cut}} = 2.5$ the results are in the same ballpark, although after rescattering the exclusive fraction is larger than the DD one. The main difference is

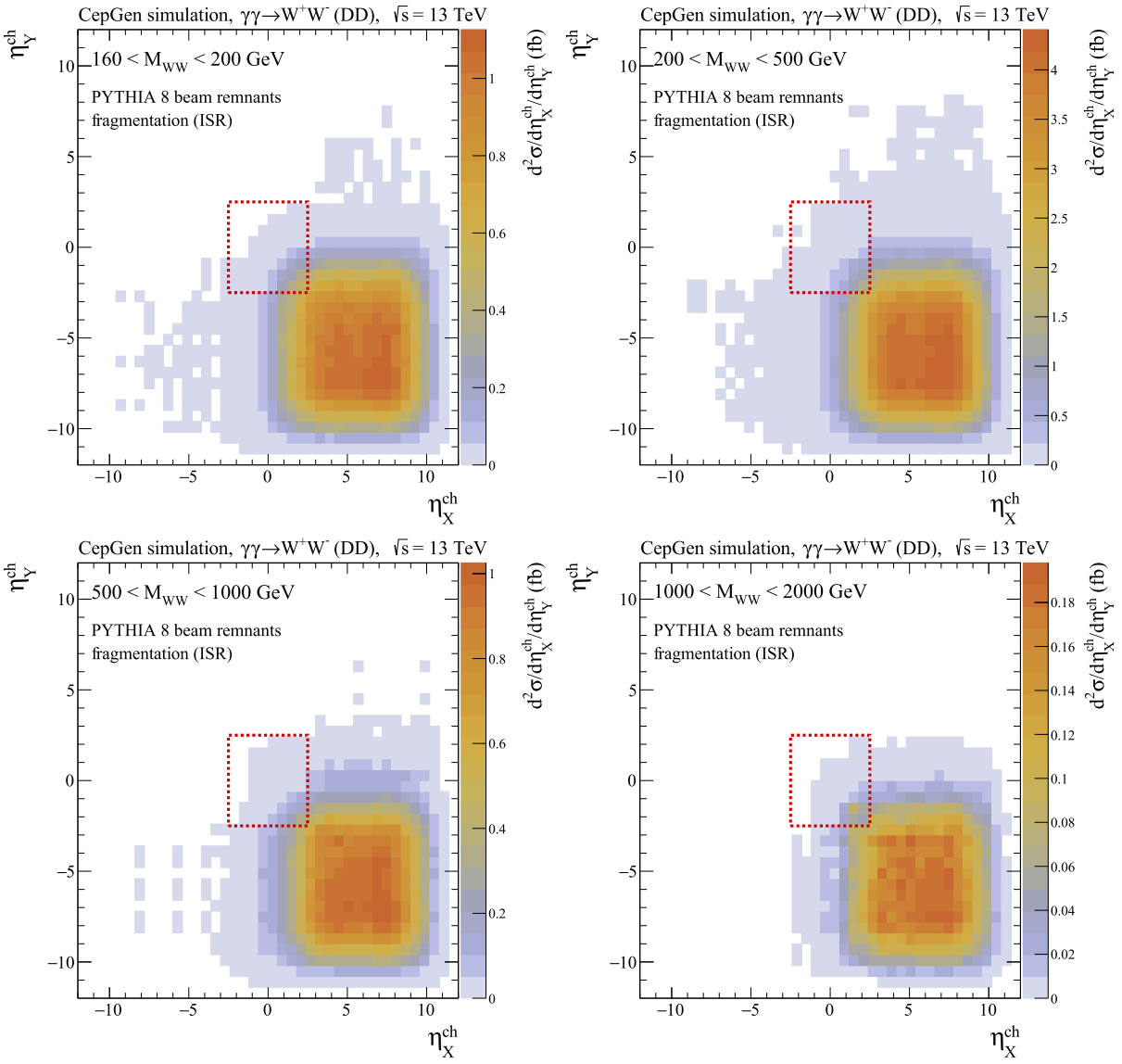

Fig. 5. Two-dimensional $(\eta_X^{\rm ch}, \eta_Y^{\rm ch})$ distribution for four different windows of M_{WW}: $(2M_W, 200\ \text{GeV})$, $(200, 500\ \text{GeV})$, $(500, 1000\ \text{GeV})$, $(1000, 2000\ \text{GeV})$. The square shows pseudorapidity coverage of ATLAS or CMS inner tracker.

Table 1
Average rapidity gap survival factor related to remnant fragmentation for *single dissociative* and *double dissociative* contributions for different ranges of M_{WW}. All uncertainties are statistical only.

Contribution	$S_{R,SD}(\lvert\eta^{\rm ch}\rvert < 2.5)$		$\left(S_{R,SD}\right)^2(\lvert\eta^{\rm ch}\rvert < 2.5)$		$S_{R,DD}(\lvert\eta^{\rm ch}\rvert < 2.5)$	
	8 TeV	13 TeV	8 TeV	13 TeV	8 TeV	13 TeV
$(2M_{WW}, 200\ \text{GeV})$	0.763(2)	0.769(2)	0.582(4)	0.591(4)	0.586(1)	0.601(2)
$(200, 500\ \text{GeV})$	0.787(1)	0.799(1)	0.619(2)	0.638(2)	0.629(1)	0.649(1)
$(500, 1000\ \text{GeV})$	0.812(2)	0.831(2)	0.659(3)	0.691(3)	0.673(2)	0.705(2)
$(1000, 2000\ \text{GeV})$	0.838(7)	0.873(5)	0.702(12)	0.762(8)	0.697(5)	0.763(6)
full range	0.782(1)	0.799(1)	0.611(2)	0.638(2)	0.617(1)	0.646(1)

for $\eta_{\rm cut} = 6.5$, where in [14] the DD contribution becomes entirely negligible. We note however that generally large ranges of dissociative masses are relevant (see e.g. Fig. 9), for which description a two-channel eikonal is not necessarily reliable. The DD component in [14] is smaller than in our case because of soft gap survival factor. The production associated with the two large masses M_X and M_Y for DD is naturally associated with smaller impact parameter and consequently the $S_{soft}(DD)$ is rather small, smaller than e.g. for the SD components.

So far we have not included the soft gap survival factors. They are relatively easy to calculate only for double elastic (DE) contribution (see e.g. [18]). For the "soft" gap survival factors we expect:

$$S_{soft}(DD) < S_{soft}(SD) < S_{soft}(DE)\ . \tag{3.4}$$

Some estimates of phase space averaged values were presented in [14]. A precise kinematics-dependent calculation of soft gap survival factor requires further studies which go, however, beyond

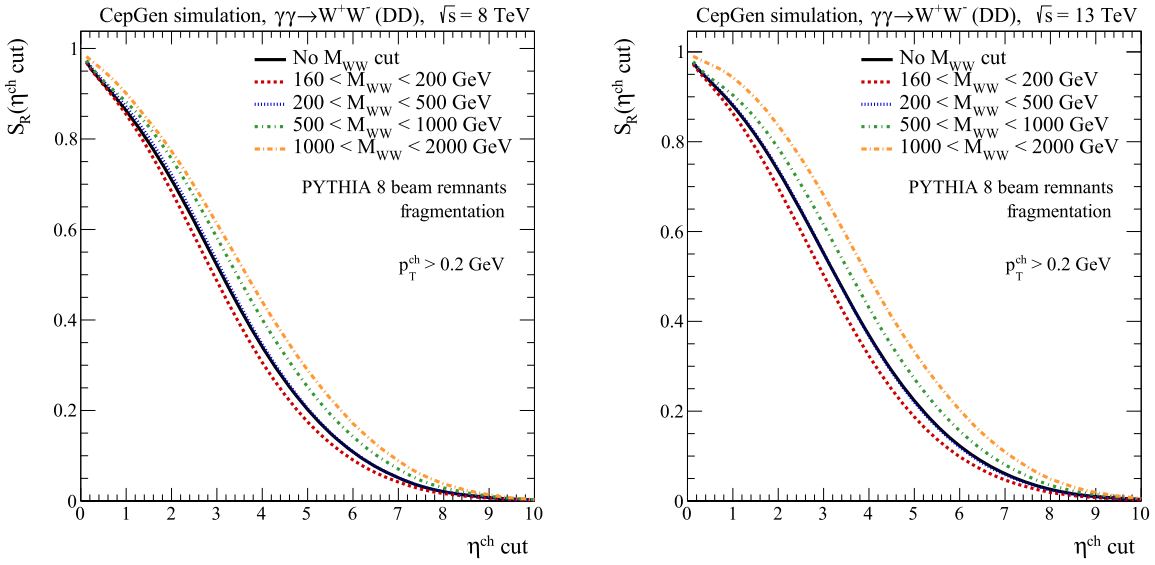

Fig. 6. Gap survival factor for double dissociation as a function of the size of the pseudorapidity veto applied on charged particles emitted from proton remnants, for the diboson mass bins defined in the text and in the figures for $\sqrt{s} = 8$ TeV (left) and 13 TeV (right).

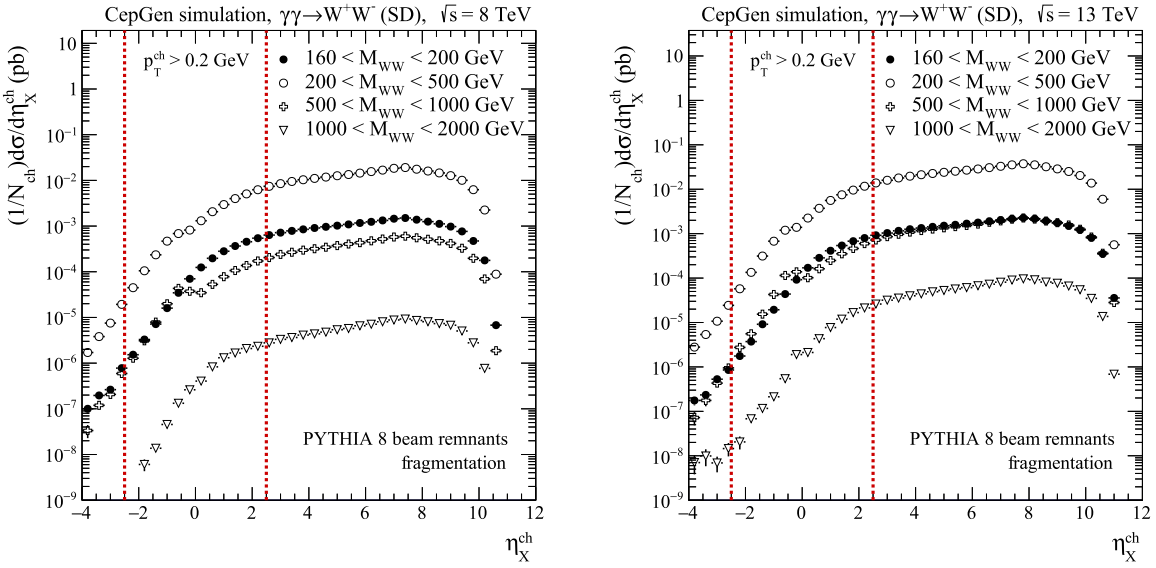

Fig. 7. η_{ch} distribution for single dissociative process for four different windows of M_{WW}: $(2M_W, 200\text{ GeV})$, $(200, 500\text{ GeV})$, $(500, 1000\text{ GeV})$, $(1000, 2000\text{ GeV})$, and for $\sqrt{s} = 8$ TeV (left) and 13 TeV (right). The lines show pseudorapidity coverage of ATLAS or CMS detector.

the scope of the letter, devoted to remnant fragmentation. We expect that the soft gap survival factors may violate the relation $S_R(DD) = (S_R(SD))^2$ for the combined (remnant+soft) rapidity gap survival factors.

4. Conclusions

In the present letter we have discussed the quantity called "remnant gap survival factor" for the $pp \to W^+W^-$ reaction initiated via photon–photon fusion. We use a recent formalism developed for the inclusive case [13] which includes transverse momenta of incoming photons.

First we have calculated the gap survival factor for single dissociative process on the parton level. In such an approach the outgoing parton (jet/mini-jet) is responsible for destroying the rapidity gap. We have discussed the role of valence and sea contributions.

Next the partonic formalism has been supplemented here by including remnant fragmentation that can spoil the rapidity gap usually used to select the subprocess of interest. We have quantified this effect by defining the remnant gap survival factor which in general depends on the reaction, kinematic variables and details of the experimental set-ups. We have found that the hadronisation only mildly modifies the gap survival factor calculated on the parton level. This may justify approximate treatment of hadronisation of remnants. We have discussed this dependence on invariant mass of the produced W^+W^- central system. We have found different values for double and single dissociative processes. In general, $S_{R,DD} < S_{R,SD}$ and $S_{R,DD} \approx (S_{R,SD})^2$. We expect that the factorisation observed here for the remnant dissociation and hadronisation will be violated when the soft processes are explicitly included. Furthermore the larger η_{cut} (upper limit on charged particles pseudorapidity), the smaller rapidity gap survival factor S_R. This holds

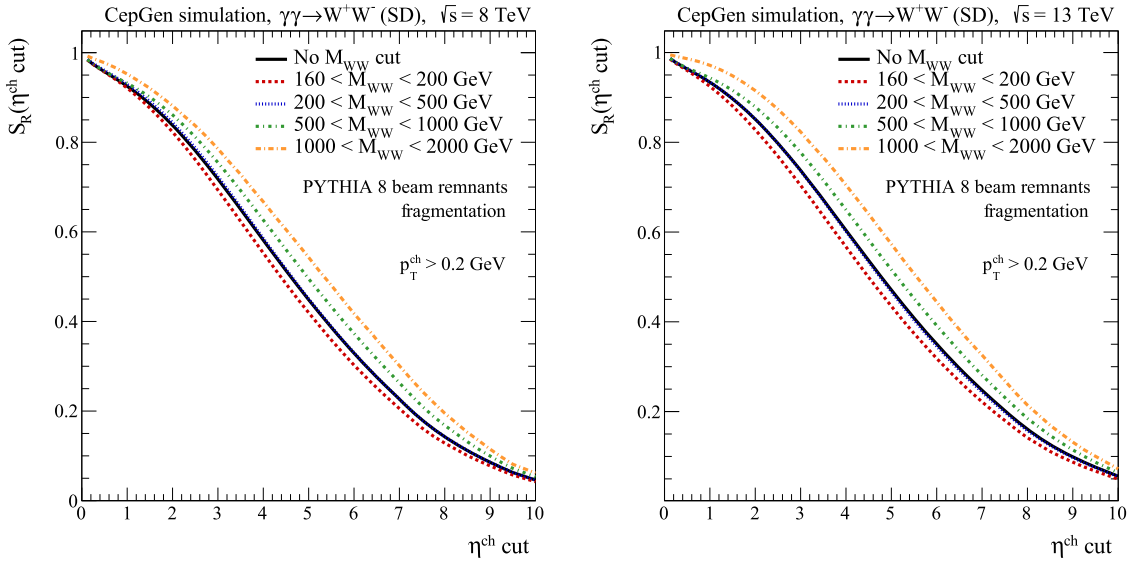

Fig. 8. Gap survival factor for single dissociation as a function of the size of the pseudorapidity veto applied on charged particles emitted from proton remnants, for the diboson mass bins defined in the text and in the figures for $\sqrt{s} = 8$ TeV (left) and 13 TeV (right).

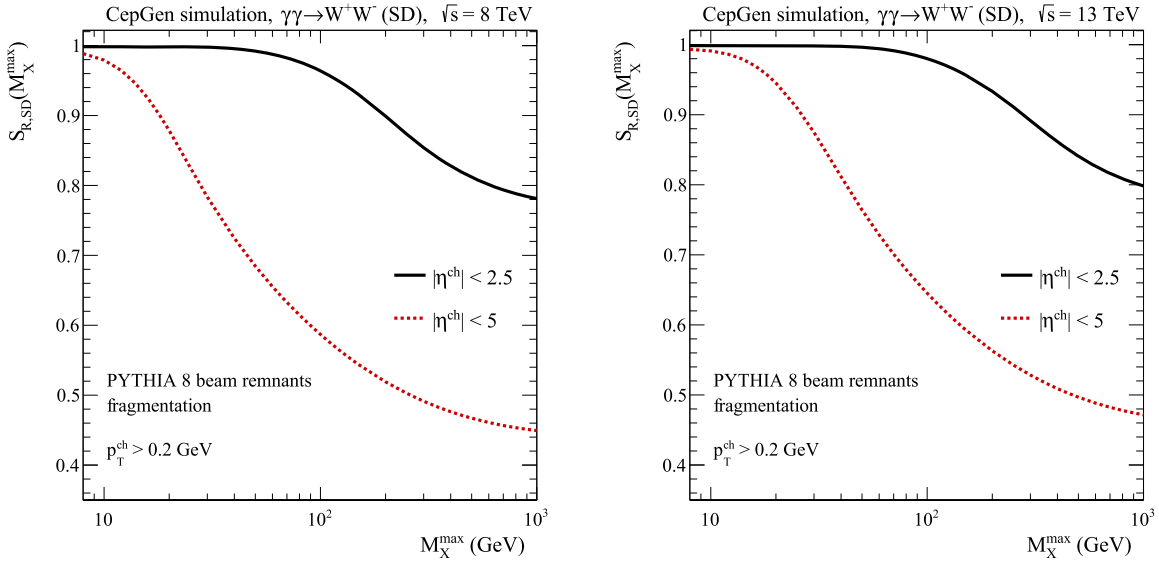

Fig. 9. Rapidity gap survival factor for $|\eta^{\mathrm{ch}}| < 2.5$ and $|\eta^{\mathrm{ch}}| < 5$ as a function of the upper limit set on M_X, the remnant system invariant mass, for single dissociation.

Table 2
Relative contribution of exclusive (Exc.), single dissociative (SD) and double dissociative (DD) contributions to photon-induced W^+W^- production at $\sqrt{s} = 13$ TeV.

Contribution	13 TeV
Inclusive	
Exc.	0.11
SD	0.44
DD	0.47
$\eta_{\mathrm{cut}} = 6.5$ ($\delta \sim 3$)	
Exc.	0.39
SD	0.35
DD	0.26
$\eta_{\mathrm{cut}} = 2.5$ ($\delta \sim 7$)	
Exc.	0.15
SD	0.58
DD	0.19

both for the double and the single dissociation. Finally the effect becomes smaller for larger collision energies. We have found that the crucial variable for S_R is (are) masses of the final hadronic remnant systems.

The present approach is a step towards a realistic modelling of gap survival in photon induced interactions and definitely requires further detailed studies and comparisons to the existing and future experimental data. In the present analyses we have neglected other effects such as soft interactions or multiple-parton interactions (see e.g. [26,27]). More detailed studies including such effects in a consistent manner will be given elsewhere.

Acknowledgements

This study was partially supported by the Polish National Science Centre grants DEC-2013/09/D/ST2/03724 and DEC-2014/15/B/ST2/02528 and by the Center for Innovation and Transfer of Natural Sciences and Engineering Knowledge in Rzeszów. We thank the

financial support from the grant of C. Royon as a Foundation Distinguished Professor. M.Ł. thanks CERN for the hospitality, where this work was finalised. We are indebted to R. Staszewski for a helpful discussion. L.F. thanks T. Sjöstrand for useful discussions in the PYTHIA 8 implementation of the beam remnants fragmentation. We are indebted to Valery Khoze and Lucian Harland Lang for a discussion on soft rapidity gap survival factors.

References

[1] S. Chatrchyan, et al., CMS, J. High Energy Phys. 01 (2012) 052, arXiv:1111.5536.
[2] S. Chatrchyan, et al., CMS, J. High Energy Phys. 11 (2012) 080, arXiv:1209.1666.
[3] G. Aad, et al., ATLAS, Phys. Lett. B 749 (2015) 242, arXiv:1506.07098.
[4] A.M. Sirunyan, et al., CMS, TOTEM, J. High Energy Phys. 07 (2018) 153, arXiv:1803.04496.
[5] M. Aaboud, et al., ATLAS, Phys. Lett. B 777 (2018) 303, arXiv:1708.04053.
[6] V. Khachatryan, et al., CMS, J. High Energy Phys. 08 (2016) 119, arXiv:1604.04464.
[7] M. Aaboud, et al., ATLAS, Phys. Rev. D 94 (2016) 032011, arXiv:1607.03745.
[8] E. Chapon, C. Royon, O. Kepka, Phys. Rev. D 81 (2010) 074003, arXiv:0912.5161.
[9] T. Pierzchała, K. Piotrzkowski, Nucl. Phys. Proc. Suppl. 179–180 (2008) 257, arXiv:0807.1121.
[10] G.G. da Silveira, L. Forthomme, K. Piotrzkowski, W. Schäfer, A. Szczurek, J. High Energy Phys. 02 (2015) 159, arXiv:1409.1541.
[11] M. Łuszczak, W. Schäfer, A. Szczurek, Phys. Rev. D 93 (2016) 074018, arXiv:1510.00294.
[12] M. Łuszczak, A. Szczurek, C. Royon, J. High Energy Phys. 02 (2015) 098, arXiv:1409.1803.
[13] M. Łuszczak, W. Schäfer, A. Szczurek, J. High Energy Phys. 05 (2018) 064, arXiv:1802.03244.
[14] L.A. Harland-Lang, V.A. Khoze, M.G. Ryskin, Eur. Phys. J. C 76 (2016) 255, arXiv:1601.03772.
[15] S.P. Baranov, O. Duenger, H. Shooshtari, J.A.M. Vermaseren, in: Workshop on Physics at HERA, Hamburg, Germany, October 29–30, 1991, 1991, pp. 1478–1482.
[16] J.D. Bjorken, Phys. Rev. D 47 (1993) 101.
[17] M. Dyndal, L. Schoeffel, Phys. Lett. B 741 (2015) 66, arXiv:1410.2983.
[18] P. Lebiedowicz, A. Szczurek, Phys. Rev. D 91 (2015) 095008, arXiv:1502.03323.
[19] J. Collins, H. Jung, in: HERA and the LHC: A Workshop on the Implications of HERA for LHC Physics. Proceedings, Part B, 2005, arXiv:hep-ph/0508280.
[20] A.D. Martin, W.J. Stirling, R.S. Thorne, G. Watt, Eur. Phys. J. C 63 (2009) 189, arXiv:0901.0002.
[21] P.E. Bosted, M.E. Christy, Phys. Rev. C 77 (2008) 065206, arXiv:0711.0159.
[22] A. Airapetian, et al., HERMES, J. High Energy Phys. 05 (2011) 126, arXiv:1103.5704.
[23] K. Abe, et al., E143, Phys. Lett. B 452 (1999) 194, arXiv:hep-ex/9808028.
[24] L. Forthomme, arXiv:1808.06059, 2018.
[25] T. Sjöstrand, S. Ask, J.R. Christiansen, R. Corke, N. Desai, P. Ilten, S. Mrenna, S. Prestel, C.O. Rasmussen, P.Z. Skands, Comput. Phys. Commun. 191 (2015) 159, arXiv:1410.3012.
[26] V.A. Khoze, A.D. Martin, M.G. Ryskin, J. Phys. G 45 (2018) 053002, arXiv:1710.11505.
[27] I. Babiarz, R. Staszewski, A. Szczurek, Phys. Lett. B 771 (2017) 532, arXiv:1704.00546.